HHS Public Access

Author manuscript

J Bone Miner Res. Author manuscript; available in PMC 2016 February 01.

Published in final edited form as:

J Bone Miner Res. 2015 October ; 30(10): 1914–1924. doi:10.1002/jbmr.2522.

Decreased Mechanical Strength and Collagen Content in SPARC-Null Periodontal Ligament is Reversed by Inhibition of Transglutaminase Activity

Jessica Trombetta-eSilva[1], **Emilie A Rosset**[1], **R Glenn Hepfer**[2], **Gregory J Wright**[2], **Catalin Baicu**[3], **Hai Yao**[1,2], and **Amy D Bradshaw**[1,3,4]

[1]Department of Craniofacial Biology, Medical University of South Carolina, Charleston, SC, USA

[2]Department of Bioengineering, Clemson University, Clemson, SC, USA

[3]Gazes Cardiac Research Institute, Division of Cardiology, Department of Medicine, Medical University of South Carolina, Charleston, SC, USA

[4]Ralph H. Johnson Department of Veterans Affairs Medical Center, Charleston, SC, USA

Abstract

The periodontal ligament (PDL) is a critical tissue that provides a physical link between the mineralized outer layer of the tooth and the alveolar bone. The PDL is composed primarily of nonmineralized fibrillar collagens. Expression of secreted protein acidic and rich in cysteine (SPARC/osteonectin), a collagen-binding matricellular protein, has been shown to be essential for collagen homeostasis in PDL. In the absence of SPARC, PDL collagen fibers are smaller and less dense than fibers that constitute WT PDL. The aim of this study was to identify cellular mechanisms by which SPARC affected collagen fiber assembly and morphology in PDL. Cross-linking of fibrillar collagens is one parameter that is known to affect insoluble collagen incorporation and fiber morphology. Herein, the reduction in collagen fiber size and quantity in the absence of SPARC expression was shown to result in a PDL with reduced molar extraction force in comparison to that of WT mice (C57Bl/6J). Furthermore, an increase in transglutaminase activity was found in SPARC-null PDL by biochemical analyses that was supported by immunohistochemical results. Specifically, collagen I was identified as a substrate for transglutaminase in PDL and transglutaminase activity on collagen I was found to be greater in SPARC-null tissues in comparison to WT. Strikingly, inhibition of transglutaminase activity in SPARC-null PDL resulted in increases in both collagen fiber thickness and in collagen content, whereas transglutaminase inhibitors injected into WT mice resulted in increases in collagen fiber thickness only. Furthermore, PDL treated with transglutaminase inhibitors exhibited increases in molar extraction force in WT and in SPARC-null mice. Thus, SPARC is proposed to act as a critical regulator of transglutaminase activity on collagen I with implications for mechanical strength of tissues.

Address correspondence to: Amy D. Bradshaw, PhD, Medical University of South Carolina, 114 Doughty St. MSC 773, Charleston, SC 29425, USA. bradshad@musc.edu.

Additional supporting information may be found in the online version of this article at the publisher's web-site.

Disclosures

All authors state that they have no conflicts of interest.

Keywords

BONE MATRIX; NONCOLLAGENOUS PROTEINS; DENTAL BIOLOGY; EXTRACELLULAR MATRIX; CROSS-LINKS

Introduction

The collagen fibers of the periodontal ligament (PDL) secure the cementum, the mineralized outer layer of the tooth, to the alveolar bone. Loss of PDL collagen fibers in periodontal disease, for example, is a contributing factor to alveolar bone destruction and tooth loss. Maintaining the integrity of the PDL collagen fibers and restoring these structures following disease treatment are essential for tooth health.[1] Thus elucidation of the cellular mechanisms that govern collagen fiber assembly, architecture, and subsequent turnover in the PDL are critical for the design of new therapies to ameliorate PDL tissue destruction and ultimately to design strategies for the regeneration of this important tissue during and following disease resolution.[2]

Secreted protein acidic and rich in cysteine (SPARC; also known as osteonectin and BM-40) is a collagen-binding matricellular protein previously shown to influence collagen fiber diameter and content.[3] SPARC-null mice exhibit osteopenia characterized by reduced osteoblast numbers and decreased rates of bone formation.[4,5] SPARC-null mice also exhibit reduced amounts of fibrillar collagen in soft connective tissues as well, including dermis and PDL.[3,6] SPARC-null PDL collagen fibers demonstrate differences in morphology characterized by lower amounts of thick collagen fibers versus WT PDL.[3] In response to LPS administration, SPARC-null mice undergo greater loss of PDL collagen fibers in comparison to WT in the absence of increased inflammatory cell infiltration after 4 weeks of LPS exposure.[7] Hence, the reduction in size and number of collagen fibers in SPARC-null PDL appears to result in a PDL that is more susceptible to degradation and/or less capable of regeneration, despite a reduction in inflammatory mediators. These results suggest that intrinsic differences in PDL collagen might be a significant factor in susceptibility to periodontal disease independent of inflammation.

A number of factors are known to influence collagen fiber diameter, including proteoglycans such as decorin and fibromodulin, other collagen family members, notably fibril associated collagens with interrupted triple helices (FACIT collagens), and intermolecular and intramolecular cross-linking of fibrillar collagens.[8–12] Transglutaminases (TGs) are a group of extracellular cross-linking proteins shown previously to demonstrate collagen cross-linking activity in vitro.[13–15] TGs are a family of proteins, eight of which have currently been identified and characterized, which are expressed in various tissues throughout the body and catalyze an irreversible covalent acyl exchange between a glutamine and a lysine.[16] The most ubiquitously expressed form of TG is tissue TG2. Recently, Wang and colleagues[12] reported that TG2 activity was necessary for the assembly of uniform, small-diameter collagen fibers deposited by corneal fibroblasts. Whereas lysyl oxidase–mediated cross-links were critical for lateral packing of collagen fibers generated by corneal fibroblasts, TG2 inhibition affected collagen fibril diameter in

this culture model. Furthermore, addition of increasing concentrations of TG2 resulted in the formation of smaller collagen fibrils in reconstituted mixtures derived from cornea. TG has also been shown to cross-link fragments of collagen I to fibronectin, in addition to other extracellular matrix (ECM) proteins such as osteopontin.[17] Pertinent to this study, SPARC was previously shown to serve as a substrate for TG in chondrocytes.[18] SPARC serves as a potent TG substrate, to the extent that a conjugated peptide derived from the first seven N-terminal amino acids of SPARC (which includes the TG donor site) has been developed as a tool to identify TG substrates and measure TG activity.[19,20]

Although evidence for TG-dependent collagen cross-linking has been shown in vitro and in bioengineered tissue scaffolds, the function of TG in vivo as a regulator of tissue architecture and in collagen cross-linking is less defined.[12–15,21,22] To test whether TG activity was altered in SPARC-null PDL, experiments in which levels of TG activity and the presence of the cross-linked epitope created by TG, N-ε-γ-glutamyl lysine, were performed in WT and in SPARC-null PDL. Furthermore, administration of a TG inhibitor was performed to determine whether decreases in collagen fiber thickness, content, and molar extraction force characteristic of SPARC-null PDL could be rescued through a reduction in TG activity in vivo. Mice were used in these studies based on availability of transgenic null animals. These results demonstrate a distinct role of TG in the regulation of collagen fiber assembly and the control of collagen fiber thickness in the PDL with significant implications in collagen biology.

Materials and Methods

Animal use and care

Homozygous C57BL/6J SPARC-null mice used in this study have global abrogation of SPARC expression as described.[23] Wild-type C57BL/6J (WT) mice were used as control. Both male and female mice from both genotypes were used in this study and were randomly assigned within genotypes. All mice were housed in the Ralph H. Johnson Veteran's Administration (VA) animal facility and were supplied with a standard diet. All animal procedures used in this study were approved by the VA Institutional Animal Care and Use Committee.

Mechanical testing of PDL

Mandibles were dissected from 1-month-old WT and SPARC-null mice (n = 9 per genotype) and a 30G wire was inserted below the crown of the first molar. The mandible was fixed from below and the wire grasped in clamps from above (Fig. 1*A*). The upper clamps were elevated at a rate of 0.017 mm/s, until the tooth was extracted from the socket. The maximum force required to remove the tooth was recorded as the molar extraction force. The same protocol was used to assess mechanical strength in mice (2 months of age) injected with BPA (n = 5 per genotype and condition).

Immunofluorescence of PDL

Jaws from SPARC-null or WT mice were fixed in 10% formalin. Following fixation, mandibles and maxillae were decalcified in 0.5M EDTA for 2 weeks and then dehydrated,

embedded in paraffin, and sectioned (5 to 7 μm). The area of the PDL represented in each of the figures was taken from similar regions of the PDL—the cervical and the middle portions of the outer PDL of the molars. All sections are longitudinal sections. Sections were mounted on glass slides and rehydrated through graded ethanol rinses. Sections were rinsed with phosphate buffered saline containing 2% Tween (PBSt) for 10 min and blocked in 3% normal donkey serum in PBSt. Slides were then incubated with antibodies generated against the N-ε–γ-glutamyl lysine crosslink epitope (1:200 dilution; Abcam Cambridge, MA) for 1 hour followed by fluorescein conjugated anti-mouse IgM secondary antibody (1:200 dilution) or avidin-fluorescein (1:200) to detect biotinylated cadaverine. Prolong anti-fade mounting medium containing DAPI (Molecular Probes, Eugene, OR, USA) was used to mount cover slips, and sections were viewed on an Olympus Confocal Microscope.

Organ culture

Mandibles and maxillae were removed from 1-month-old WT and SPARC-null mice and dissected free of muscle and loose tissue. Jaws from a single mouse were placed in one well of a 24-well plate with 1 mL of growth media (DMEM 10% FCS 0.2% primocin, 50 μg/mL ascorbate). Additional factors such as 5-(Biotinamido) pentylamine (BPA; 2 μM), NC9 (80 μM), or equal volumes of vehicle control, were added to the growth media as warranted by experimental design. Jaws were then incubated at 37°C, with 5% CO_2 for 24, 48, or 72 hours prior to molar extraction. Molars from a single mouse (12 teeth) were placed in 100 μL of 2.5% SDS in dH_2O, supplemented with protease inhibitors (Roche Indianapolis, IN) or were decalcified as described above (Immunofluorescence of PDL) and processed for immunohistochemistry. Teeth were stored at –80°C overnight and then tumbled at 4°C for 4 hours to extract PDL protein. Teeth extracted in SDS buffer were boiled, vortexed, and then boiled for an additional 5 min. After boiling, these samples were centrifuged at 10,000*g* for 10 min, and the supernatants used for determination of total protein concentration by bicinchoninic acid (BCA) analysis and subsequent immunoblot or immunoprecipitation analysis.

Immunoblots

Equal amounts of protein were separated by SDS-PAGE analysis followed by staining with Coomassie brilliant blue to confirm equal loading or transferred to nitrocellulose membranes. Membranes were blocked in 3% bovine serum albumin in Tris-buffered saline with 0.2% Tween (TBST) for 1 hour at room temperature. Membranes were then incubated with primary antibodies, either anti-collagen α1(I) (1:10,000 dilution; MD Biosciences St. Paul, MN) or avidin–horseradish peroxidase (HRP) (to detect BPA) (Vector Laboratories Burlingame, CA) followed by appropriate secondary antibodies (Vector Laboratories) and detection with chemiluminescence reagent (Pierce Grand Island, NY). The intensity of bands generated from TG modification by labeled donor substrates was quantified with NIH Image J software.

Immunoprecipitation

Equal amounts of protein extracted from WT and SPARC-null teeth were tumbled overnight with 5 μg of collagen α1(I) antibody (MD Biosciences) at 4°C or 5 μg of control IgG.

Protein A/G beads were then added and tumbled at 4°C. Bead/immunocomplexes were pelleted, washed three times with radioimmunoprecipitation assay (RIPA) buffer and boiled for 5 min with 40 μL of Laemmli buffer. Proteins were then separated on 3% to 8% SDS-PAGE gels (Novex, Life Sciences Grand Island, NY) and probed with either anti-collagen I antibodies or with avidin-HRP for detection of BPA incorporation. No proteins were detected by avidin-HRP antibodies in control pull down with control IgG.

RNA isolation from PDL and reverse-transcription PCR

Twelve molars from four WT and six SPARC-null mice were extracted in 1 mL of Trizol and frozen in liquid N_2. Samples were thawed on ice and incubated with 24 parts chloroform to 1 part isoamyl alcohol. Teeth were then centrifuged 10 min at 10,000 X g the top layer was transferred to a fresh tube, and the teeth were discarded with the organic layer. RNA was precipitated with isopropyl alcohol. RNA pellets were resus-pended in 200 μL of RNA solution (198 μL of water, 2 μL of 100 mM magnesium chloride, and 2 μL of DNase per sample). Samples were heated in a 37°C water bath for 25 min, followed by 5 min in a 95°C heat block. Quantitation of mRNA used a one-step reverse transcription (RT)-PCR kit (QuantiTect SYBR Green RT-PCR Kit; QIAGEN Sciences, Gaithersburg, MD, USA) and a CFX96 Real-Time System C1000 Thermal Cycler (BioRad, Hercules, CA, USA). Samples were run in triplicate using the gene-specific primer sets shown in Supporting Table 1. The amount of mRNA in individual samples was calculated from a standard curve that was generated for each run using a dilution series derived from a sample of total PDL RNA. The relative level of each mRNA was calculated by normalizing to the amount of 18S rRNA in each sample.[24]

In vivo inhibition of TG with BPA injections

Sixteen SPARC-null and 16 WT 1-month-old male mice were used. Eight mice of each genotype were anesthetized with 1000 mL/min of O_2 and 5% isoflurane, and then injected with either 2 μL of BPA (2 mM in DMSO) or 2 μL of DMSO vehicle (Invitrogen) in the palatal gingiva between the right maxillary first and second molars. Mice received injections thrice weekly over a 2-week time period. A second set of mice (n = 10 per genotype) were injected for mechanical testing with the exception that right mandibular first and second molars were injected. At termination, jaws were collected from each mouse and processed for histology or mechanical testing.

Histological analysis of collagen morphology and collagen volume fraction analysis

Mandibles and maxillae were removed from SPARC-null and WT mice treated with BPA or DMSO only and processed for histology as described above (Immunfluorescence of PDL). Four mice per genotype and condition were analyzed. Picrosirius red (PSR) staining was performed as described.[3] Sections were analyzed with an Olympus Bx50WI scope equipped with Infinity2 Capture software. Images from PSR-stained sections were quantified using a Visiopharm Integrator System (version 3.2.9.0). Parameters were set in this program to measure the total area of the PDL and the area of total collagen, thick collagen fibers, and thin collagen fibers. At least five fields per mouse and four animals per genotype and treatment contributed to the quantification. Mean, SD, and standard error of

the mean (SE) were calculated for each condition. Values >2SD from the mean were removed as outliers. Treated and control animals were analyzed using a Student's *t* test analysis; *p* values <0.05 were considered significant.

Statistical analysis

The number of animals used for each experiment was based on previous results, with the primary determinant being the magnitude of difference in collagen volume fraction between WT and SPARC-null PDL. For comparisons within genotypes, a paired Student's *t* test was used to calculate *p* values. Comparisons between genotypes with one condition were analyzed using a Student's *t* test. For comparisons between genotypes with more than one condition, ANOVA followed by Tukey test was used to calculate *p* values. For all analyses, $p < 0.05$ was considered statistically significant.

Results

Decreases in collagen content and fiber thickness correlates with decreases in mechanical strength in SPARC-null PDL

Previously, decreases in collagen content and fiber thickness were reported in SPARC-null versus WT PDL.[3] To determine whether these decreases affected mechanical strength of the PDL, tooth extraction forces were measured for SPARC-null and WT mice. As shown in Fig. 1*A*, mandibles isolated from each genotype were secured to a clamp attached to a high-sensitivity load cell and the first molar pulled from above as described in Materials and Methods. Using this device, the force required to extract teeth from SPARC-null jaws was found to be significantly less than that required to remove teeth from WT mandibles (Fig. 1*B*). Representative PSR-stained images of PDL from 1-month-old WT and SPARC-null mice are shown to demonstrate the reduction in collagen content and collagen fiber thickness as previously reported Reference #3 in SPARC-null mice (Fig. 1*B*). A 64% reduction in tooth extraction force was found in SPARC-null mice versus WT ($p < 0.001$). Examination of extracted teeth revealed that tissue failure occurred within the PDL in both WT and SPARC-null samples. Thus, differences in collagen content and architecture in the absence of SPARC expression resulted in a PDL with reduced mechanical strength.

Increased N-ε-γ-glutamyl-lysyl cross-links in SPARC-null PDL

One factor known to influence collagen fiber architecture is the formation of covalent cross-links that result in insoluble incorporation of collagen into the extracellular matrix (ECM). TGs form covalent cross-links between proteins in the extracellular space through catalysis of a N-ε-γ-glutamyl lysyl bond on adjacent proteins. To detect the presence of TG activity in the PDL, sections from WT (Fig. 2*A*, *C*) and SPARC-null (Fig. 2*B*, *D*) mice were stained with antibodies generated against the bond formed by TG. Immunoreactivity was detected in WT PDL and appeared in a punctate pattern around PDL fibroblasts (Fig. 2*C*, red arrows). Immunoreactivity was also detected in SPARC-null tissues, in which the signal appeared to be more robust than that in WT tissues. In addition, the pattern of staining was more localized to discrete areas on and around fibroblasts (Fig. 2*D*).

Analyses of TG activity in organ culture

Mechanisms of collagen fiber assembly are difficult to characterize using traditional tissue culture because of the lack of a 3D environment that can provide mechanical forces essential for ECM assembly. Notably, TG activity in 2D cultures was found to be significantly less than in organ culture and with differential incorporation of TG substrates (Trombetta-eSilva and Bradshaw, unpublished data). To circumvent these limitations, an organ culture system was developed to preserve the intrinsic mechanical environment of PDL fibroblasts as depicted in Fig. 3*A*. To confirm that PDL maintained structural integrity in this organ culture system, teeth were extracted from WT and SPARC-null mice after 24 and 48 hours in culture (Fig. 3*B*). Forces required to extract teeth from cultured jaws did not diminish over 48 hours and were similar to that of freshly isolated tissue (time 0). SPARC-null teeth, however, consistently showed decreased mechanical integrity as evidenced by the lesser forces required to pull teeth from SPARC-null jaws versus WT teeth (Fig. 3*B*).

To detect TG activity in situ, organ cultures were incubated with 5-(Biotinamido) pentylamine (BPA). BPA is a biotin labeled pentylamine that can serve as a free amine group in the transamidation reaction catalyzed by TG.[25] BPA is covalently cross-linked by TG activity to a substrate protein containing a glutamine donor, and as such serves as an inhibitor to the cross-link formation, and also serves as a labeling compound, which will modify the donor glutamine of specific TG substrates with a biotin group. Detection of BPA incorporation with fluoresceinconjugated secondary antibodies was performed in sections of PDL grown in organ culture for 24 hours. As shown in Fig. 3*C*, apparent greater fluorescence intensity was associated with SPARC-null PDL in comparison to that of WT, consistent with increased TG activity in the absence of SPARC expression.

PDL proteins from jaws grown in organ culture incubated with BPA or control vehicle were separated by SDS-PAGE and probed with avidin-HRP to detect proteins modified by TG in WT and SPARC-null conditions. Shown in Fig. 4*A*, proteins from SPARC-null PDL organ culture demonstrated greater incorporation of BPA in comparison to those of WT tissues. Equal loading of proteins from each condition, determined by BCA analysis, was confirmed by Coomassie stain (Fig. 4*B*). Interestingly, although some proteins appeared to have increased intensity in the absence of SPARC (Fig. 4*A*, arrows), at least one band showed decreased intensity in SPARC-null versus WT (Fig. 4*A*, arrowhead). Overall, quantification of four separate organ cultures showed that BPA-incorporation was greater in proteins separated by SDS-PAGE from SPARC-null PDL in comparison to total proteins from WT (Fig. 4*C*). To provide evidence that BPA incorporation into WT and SPARC-null PDL proteins was specific to TG activity, organ culture experiments were carried out using a TG-specific inhibitor, NC9. NC9 was shown to be an irreversible inhibitor of TG activity.[26,27] Incubation of NC9 with BPA decreased the amount of BPA incorporated into proteins (Supporting Fig. 1).

Greater BPA modification of Collagen I by TG in SPARC-null PDL

Given the alterations in collagen fiber morphology in SPARC-null PDL, experiments were performed to determine whether collagen I served as a substrate for TG in PDL and whether expression of SPARC affected BPA incorporation to collagen I. As shown in Fig. 5, pull-

down experiments using anti-collagen I antibodies revealed that collagen I was a substrate that was modified with BPA in PDL organ culture. In addition, collagen I pulled down from SPARC-null PDL protein extracts consistently demonstrated increased incorporation of BPA versus that from WT PDL despite lower overall levels of extracted collagen.

TG expression in PDL

To determine which members of the TG family might contribute to increases in N-ε-γ-glutamyl immunoreactivity indicative of SPARC-null PDL, RT-PCR analysis with sequence specific primers was performed. Evidence for the expression of mRNA encoding TG2, TG3, TG4, TG5, and Factor XIII-A were found in samples from WT and SPARC-null PDL. No differences between the levels of mRNA encoding TG2, TG3, and TG4 were found in WT versus SPARC-null samples (Fig. 6C, D). Of the mRNAs detected, those encoding TG5 were detected at higher levels in WT samples, whereas levels of mRNA encoding Factor XIII-A were higher in SPARC-null samples (Fig. 6*A*, *B*). Given the broad connective tissue expression of TG2 and previous associations with collagen cross-link formation,[12] this family member was also assessed at the protein level. Western blot analysis using anti-TG2 antibodies confirmed protein expression of TG2 in PDL; however, no differences in levels of protein between WT and SPARC-null mice were found (Fig. 6*E*). mRNAs encoding TG1, TG6, and TG7 were not detected by RT-PCR in samples of PDL.

Inhibitors of TG restore thick collagen fibers and content in SPARC-null PDL

In the event that smaller collagen fibers and decreased collagen content in the absence of SPARC is dependent upon increases in TG activity, then inhibitors of TG are anticipated to influence collagen fiber architecture when delivered in vivo. BPA was injected every other day, between the first and second maxillary molar of WT and SPARC-null mice, for 2 weeks. Analysis of PSR-stained sections revealed that the vehicle, DMSO, caused some PDL damage, as indicated by a decrease in the percent of thick collagen (red/yellow fibers) as compared to previous baseline values, particularly in SPARC-null mice (Fig. 7*A*). [7] However, the sections derived from BPA-injected jaws appeared to have an increased amount of thick collagen as compared to the DMSO controls in both WT and SPARC-null conditions (Fig. 7*A*). When compared by independent, blinded viewers, SPARC-null BPA-injected jaws appeared to have noticeably more PDL collagen than SPARC-null DMSO controls and were difficult to distinguish from WT sections. SPARC-null DMSO-injected PSR-stained sections were distinguishable from WT sections and regarded as having less overall collagen, in association with reduced levels of thick collagen (Fig. 7*A*).

To confirm these observations, total collagen volume fraction and percent of thick collagen were quantified from PSR-stained sections by histomorphometry analysis (Fig. 7*B, C*). The percent of thick collagen was significantly increased in SPARC-null BPA-injected sections versus DMSO controls (Fig. 7*B*). In addition, SPARC-null BPA-injected PDL also exhibited significant increases in total collagen volume fraction as compared to control PDL (Fig. 7*C*). WT mice injected with BPA also demonstrated a significant increase in the percentage of thick collagen versus WT DMSO controls, although total collagen volume fraction were not significantly increased by BPA injection in WT mice. Hence, BPA injections increased total

and thick collagen volume fraction in SPARC-null PDL and brought these levels within range of that of WT mice.

Mechanical testing was performed on molars from BPA-injected WT and SPARC-null mice to determine whether inhibition of TG activity affected mechanical properties of PDL. As shown in Fig. 7*D*, WT and SPARC-null BPA-injected molars required stronger forces for extraction than vehicle-treated molars. Forces required to extract WT and SPARC-null teeth treated with BPA or vehicle control were slightly higher than those required to extract molars from mice at 1 month of age (Fig. 1*B*), likely due to the increased age of the mice used for injection (10 weeks). Increases in mechanical force required to extract molars exposed to BPA indicate that inhibition of TG activity enhances collagen fiber formation and mechanical strength of the ECM.

Discussion

Given the deficits in collagen volume fraction, susceptibility to periodontal disease, and decreased mechanical strength of PDL in SPARC-null mice, cellular mechanisms of the role of SPARC in collagen homeostasis in PDL merited investigation. Collagen cross-links are one essential aspect of insoluble collagen incorporation that influences collagen fiber morphology and tissue properties. SPARC is an established substrate of TG, acting as a glutamine donor.[18] We report herein apparent increases in immunostaining for N-ε-γ glutamyl lysine, the cross-link catalyzed by TG, in SPARC-null versus WT PDL. In addition, a novel organ culture system was used to demonstrate an increase in BPA modification of collagen I by TG in the absence of SPARC expression. Differences in collagen morphology in SPARC-null PDL, most notably the reduction in collagen fiber size and amounts of collagen, were rescued by inhibition of TG activity in vivo. In addition, inhibition of TG activity increased mechanical strength of PDL in WT and SPARC-null mice. Our data provide evidence for a function of TG in fibrillar collagen assembly in vivo and the regulation of this activity by SPARC in PDL.

TG has been shown to catalyze ECM cross-linking and has been used in the development of bioengineered scaffolds.[21] Thus, previous evidence supported a function of TG in stabilizing and cross-linking ECM proteins; however, whether TG activity was critical in collagen fiber assembly in vivo was not established. Our current studies show that the absence of SPARC was associated with increased TG activity and smaller collagen fibrils, consistent with results by Wang and colleagues[12] that showed inhibition of TG activity increased collagen fibril diameter in ECM assembled by cornea fibroblasts. Assembly of an insoluble fibronectin network has been shown to play a critical role in collagen ECM assembly in cultured cells.[28] TG2 cross-linking of fibronectin is continuous during fibronectin fibril assembly.[29] TG2 increases insoluble fibronectin incorporation, and increases the density of fibronectin fibrils in proportion to the cell surface.[30] Recently, Factor XIII-A was shown to be required for the incorporation of soluble plasma fibronectin into insoluble ECM assembled by osteoblast cultures. In line with results reported herein, inhibition of TG activity was shown to also result in increases in collagen fibril diameter in treated osteoblast cultures.[31] One possibility is that the absence of SPARC expression influences TG activity on fibronectin as well and thus affects collagen fibril assembly

secondarily. In PDL organ culture, our data showed that collagen I serves as a substrate for TG. Future studies that explore the relationship between TG-dependent cross-linking of fibronectin with regard to collagen assembly will yield interesting insights.

Until recently, many of the TG family members were thought to have restricted tissue-specific expression patterns. For example, expression of TG4, previously identified as a prostate-specific TG, has been reported in vascular tissues.[32] RT-PCR analysis of TG expression in PDL revealed mRNA expression of TG2, TG3, TG4, TG5, and Factor XIII-A. Whether TG5 or Factor XIII-A, the two TGs with alternate expression patterns between SPARC-null and WT PDL, have differential substrate specificity for specific collagens remains to be determined. Substrate specificity and distinct roles of each of these TGs in ECM assembly will be of interest in future studies. We carried out in vitro TG activity assays using total protein from PDL and liver extracted from WT and SPARC-null mice to determine whether the absence of SPARC might directly modulate TG activity (Trombetta-eSilva and Bradshaw, unpublished). However, no differences in levels of TG activity were detected using in vitro assays based on TG modification of casein. We interpret these results to reflect that SPARC does not directly inhibit intrinsic activity of TGs but instead influences substrate specificity in the extracellular milieu. As shown in Fig. 4*A* (arrow), at least one protein band present in SPARC-null PDL exhibited reduced incorporation of BPA versus WT, which supports the concept that SPARC influences substrate specificity rather than overall TG activity.

The PDL is a unique connective tissue that is highly vascularized and exposed to persistent tension as the collagen fibers weave into both the alveolar bone and cementum. The fibroblasts in PDL align perpendicular to the tooth axis, and secrete collagen in an aligned manner. Because of the high structural order and exposure to unique mechanical stimuli, PDL fibroblasts cultured in 2D have an altered phenotype to that in vivo. Accordingly, only minimal TG activity could be detected in 2D PDL fibroblast cultures (Trombetta-eSilva and Bradshaw, unpublished). Therefore, an organ culture model was established as an ex vivo system that would maintain PDL fibroblasts in the highly ordered arrangement seen in vivo and maintain some the mechanical forces of PDL. In this system, TG activity, as monitored by protein incorporation of BPA, was detected in both WT and SPARC-null conditions.

There is a possibility that increased BPA incorporation of collagen I in SPARC-null PDL does not exclusively reflect collagen cross-links, but instead might include other types of TG modification such as serotonylation.[33] In our experiments, BPA acted as a free amine. Free amines are also present in vivo, one example being serotonin.[34] Importantly, serotonylation/monoaminylation catalyzed by TG activity in platelets has been shown to increase protein-protein aggregation by integrating clotting factors such as von Willebrand factor, thrombospondin, and fibronectin.[35] Possibly, TG activity in PDL and in other tissues might facilitate ECM assembly through increasing protein-protein interaction through posttranslational modifications such as serotonylation. We also detected a number of proteins in PDL extracts that incorporated BPA in addition to collagen I. Possibly, other proteins that facilitate ECM assembly, such as fibronectin and proteoglycans, might be differentially modified by TG activity in the absence of SPARC and might contribute to changes in ECM collagen fiber morphology. Future work to investigate modifications of

collagen and other ECM components mediated by TG will be an important line of investigation.

Proteins that are cross-linked by TG are predicted to shift in molecular weight. We have been unable to detect shifts in the molecular weight of SPARC in WT PDL by Western blot that might be expected in the event that SPARC was cross-linked to other ECM proteins. However, high molecular weight insoluble forms of ECM proteins are highly difficult to resolve by SDS-PAGE analysis. Because SPARC is a collagen-binding protein, our current hypothesis is that SPARC bound to collagen reduces TG accessibility to available glutamines (and or lysines) so that TG modification of collagen is decreased. Recently, Kalamajski and colleagues[36] reported that fibromodulin, a collagen-binding small leucine rich protein (SLRP), acts to limit lysyl oxidase modification of collagen I and thus reduces collagen cross-linking mediated by lysyl oxidase. Differences in collagen fibril architecture in fibromodulin-null mice were attributed to increases in collagen cross-linking of the C-telopeptide of collagen α1(I). To date, no detectable changes in the lysyl oxidase–mediated cross-linking of collagen in SPARC-null mice have been reported. A preliminary study of dermal collagen revealed no significant differences in lysyl oxidase–dependent cross-links in SPARC-null versus WT mice (Bradshaw AD, unpublished work). Nonetheless, inhibition of TG activity had a significant effect on collagen fiber thickness in WT and more so in SPARC-null PDL, consistent with TG activity being the primary determinant of smaller collagen fibril morphology in the absence of SPARC.

Inhibition of TG activity increased the force required to extract teeth in WT and in SPARC-null mice. The conclusion that increases in collagen fiber thickness, and in SPARC-null PDL an increase in total collagen, result in a PDL with increased mechanical strength appears to be the most straightforward interpretation. Generally, increases in collagen cross-links have been associated with increases in mechanical strength and increases in tissue stiffness.[37] Hence, inhibition of TG-dependent cross-linking associated with increased mechanical strength of a tissue might appear counterintuitive. One explanation might reside in the evidence that greater TG activity was linked to reduced collagen fiber thickness. Perhaps smaller collagen fibers provide less mechanical strength regardless of increased cross-linking. In addition, the question of how collagen cross-links directly impact mechanical strength and stiffness is complex. For example, Fessel and colleagues[38] recently reported that increases in tissue strength and stiffness frequently associated with increases in advanced glycation end-product (AGE) cross-links did not impact stiffness of individual collagen fibrils in tendon. Differences in molecular sliding between supramolecular collagen structures were identified as an important factor in mediating the effects of AGE-modified collagen cross-links. Hence, the nature of the molecular basis by which TG activity determines collagen fiber thickness and mechanical strength will be insightful.

Supplementary Material

Refer to Web version on PubMed Central for supplementary material.

Acknowledgments

This work was supported by NIH F30DE023009-01 (J.T-eS.), NIH predoctoral fellowship award F31DE023482 (GJW), Veteran's Administration Merit Award 1I01BX001385-01A1 (ADB), and NIH R01DE021134 (HY).

Authors' roles: JTE, CB, HY, ADB designed the study. JTE, EAR, RGH, GJW, and CB performed the study, collected and analyzed data. JTE, EAR, ADB interpreted data. JTE and ADB drafted the paper. JTE, CB, HY, and ADB critically revised and approved the final version of the manuscript and agreed to be accountable for all aspects of the work. JTE and ADB take responsibility for the integrity of the data analysis.

References

1. Beertsen W, McCulloch CA, Sodek J. The periodontal ligament: a unique, multifunctional connective tissue. Periodontology. 1997; 13:20–40. 2000.
2. Rios HF, Lin Z, Oh B, Park CH, Giannobile WV. Cell- and gene-based therapeutic strategies for periodontal regenerative medicine. J Periodontol. 2011; 82(9):1223–37. [PubMed: 21284553]
3. Trombetta JM, Bradshaw AD. SPARC/osteonectin functions to maintain homeostasis of the collagenous extracellular matrix in the periodontal ligament. J Histochem Cytochem. 2010; 58(10): 871–9. [PubMed: 20566756]
4. Delany AM, Kalajzic I, Bradshaw AD, Sage EH, Canalis E. Osteonectin-null mutation compromises osteoblast formation, maturation, and survival. Endocrinology. 2003; 144(6):2588–96. [PubMed: 12746322]
5. Delany AM, Amling M, Priemel M, Howe C, Baron R, Canalis E. Osteopenia and decreased bone formation in osteonectin-deficient mice. J Clin Invest. 2000; 105(7):915–23. [PubMed: 10749571]
6. Bradshaw AD, Puolakkainen P, Dasgupta J, Davidson JM, Wight TN, Sage EH. SPARC-null mice display abnormalities in the dermis characterized by decreased collagen fibril diameter and reduced tensile strength. J Invest Dermatol. 2003; 120(6):949–55. [PubMed: 12787119]
7. Trombetta-Esilva J, Yu H, Arias DN, Rossa C Jr, Kirkwood KL, Bradshaw AD. LPS induces greater bone and PDL loss in SPARC-null mice. J Dent Res. 2011; 90(4):477–82. [PubMed: 21191126]
8. Chen S, Birk DE. The regulatory roles of small leucine-rich proteoglycans in extracellular matrix assembly. FEBS.J. 2013; 280(10):2120–37. [PubMed: 23331954]
9. van der Rest M, Garrone R. Collagen family of proteins. FASEB.J. 1991; 5(13):2814–23. [PubMed: 1916105]
10. Orgel JP, San Antonio JD, Antipova O. Molecular and structural mapping of collagen fibril interactions. Connect Tissue Res. 2011; 52(1):2–17. [PubMed: 21182410]
11. Connizzo BK, Yannascoli SM, Soslowsky LJ. Structure-function relationships of postnatal tendon development: a parallel to healing. Matrix Biol. 2013; 32(2):106–16. [PubMed: 23357642]
12. Wang L, Uhlig PC, Eikenberry EF, Robenek H, Bruckner P, Hansen U. Lateral growth limitation of corneal fibrils and their lamellar stacking depend on covalent collagen cross-linking by transglutaminase-2 and lysyl oxidases, respectively. J Biol Chem. 2014; 289(2):921–9. [PubMed: 24265319]
13. Mosher DF. Cross-linking of fibronectin to collagenous proteins. Mol Cell Biochem. 1984; 58(1-2):63–8. [PubMed: 6143254]
14. Fortunati D, Chau DY, Wang Z, Collighan RJ, Griffin M. Cross-linking of collagen I by tissue transglutaminase provides a promising biomaterial for promoting bone healing. Amino Acids. 2014; 46(7):1751–61. [PubMed: 24710705]
15. Bowness JM, Folk JE, Timpl R. Identification of a substrate site for liver transglutaminase on the aminopropeptide of type III collagen. J Biol Chem. 1987; 262(3):1022–4. [PubMed: 2879837]
16. Iismaa SE, Mearns BM, Lorand L, Graham RM. Transglutaminases and disease: lessons from genetically engineered mouse models and inherited disorders. Physiol Rev. 2009; 89(3):991–1023. [PubMed: 19584319]
17. Kaartinen MT, Pirhonen A, Linnala-Kankkunen A, Maenpaa PH. Cross-linking of osteopontin by tissue transglutaminase increases its collagen binding properties. J Biol Chem. 1999; 274(3):1729–35. [PubMed: 9880554]

18. Aeschlimann D, Kaupp O, Paulsson M. Transglutaminase-catalyzed matrix cross-linking in differentiating cartilage: identification of osteonectin as a major glutaminyl substrate. J Cell Biol. 1995; 129(3):881–92. [PubMed: 7730416]
19. Khew S, Panengad P, Raghunath M, Tong Y. Characterization of amine donor and acceptor sites for tissue type transglutaminase using a sequence from the C-terminus of human fibrillin-1 and the N-terminus of osteonectin. Biomaterials. 2010; 31(16):4600–8. [PubMed: 20223517]
20. Khew S, Yang Q, Tong Y. Enzymatically crosslinked collagen-mimetic dendrimers that promote integrin-targeted cell adhesion. Biomaterials. 2008; 29(20):3034–45. [PubMed: 18420267]
21. Damodaran G, Collighan R, Griffin M, Pandit A. Tethering a laminin peptide to a crosslinked collagen scaffold for biofunctionality. J Biomed Mater Res A. 2009; 89(4):1001–10. [PubMed: 18478551]
22. Piercy-Kotb SA, Mousa A, Al-Jallad HF, et al. Factor XIIIA transglutaminase expression and secretion by osteoblasts is regulated by extracellular matrix collagen and the MAP kinase signaling pathway. J Cell Physiol. 2012; 227(7):2936–46. [PubMed: 21959563]
23. Norose K, Clark J, Syed N, et al. SPARC deficiency leads to early-onset cataractogenesis. Invest Ophthalmol Vis Sci. 1998; 39(13):2674–80. [PubMed: 9856777]
24. Spruill LS, McDermott PJ. Regulation of c-jun mRNA expression in adult cardiocytes by MAP kinase interacting kinase-1 (MNK1). FASEB. J. 2006; 20(12):2133–5. [PubMed: 16940435]
25. Nurminskaya M, Kaartinen MT. Transglutaminases in mineralized tissues. Front Biosci. 2006; 11:1591–606. [PubMed: 16368540]
26. Al-Jallad HF, Myneni VD, Piercy-Kotb SA, et al. Plasma membrane factor XIIIA transglutaminase activity regulates osteoblast matrix secretion and deposition by affecting microtubule dynamics. PLoS One. 2011; 6(1):e15893. [PubMed: 21283799]
27. Caron NS, Munsie LN, Keillor JW, Truant R. Using FLIM-FRET to measure conformational changes of transglutaminase type 2 in live cells. PLoS One. 2012; 7(8):e44159. [PubMed: 22952912]
28. Li S, Van Den Diepstraten C, D'Souza SJ, Chan BM, Pickering JG. Vascular smooth muscle cells orchestrate the assembly of type I collagen via alpha2beta1 integrin, RhoA, and fibronectin polymerization. Am J Pathol. 2003; 163(3):1045–56. [PubMed: 12937145]
29. Verderio E, Nicholas B, Gross S, Griffin M. Regulated expression of tissue transglutaminase in Swiss 3T3 fibroblasts: effects on the processing of fibronectin, cell attachment, and cell death. Exp Cell Res. 1998; 239(1):119–38. [PubMed: 9511731]
30. Akimov S, Belkin A. Cell-surface transglutaminase promotes fibronectin assembly via interaction with the gelatin-binding domain of fibronectin: a role in TGFbeta-dependent matrix deposition. J Cell Sci. 2001; 114(Pt 16):2989–3000. [PubMed: 11686302]
31. Cui C, Wang S, Myneni VD, Hitomi K, Kaartinen MT. Transglutaminase activity arising from Factor XIIIA is required for stabilization and conversion of plasma fibronectin into matrix in osteoblast cultures. Bone. 2014; 59:127–38. [PubMed: 24246248]
32. Johnson KB, Petersen-Jones H, Thompson JM, et al. Vena cava and aortic smooth muscle cells express transglutaminases 1 and 4 in addition to transglutaminase 2. Am J Physiol Heart Circ Physiol. 2012; 302(7):H1355–66. [PubMed: 22307675]
33. Hummerich R, Thumfart JO, Findeisen P, Bartsch D, Schloss P. Transglutaminase-mediated transamidation of serotonin, dopa-mine and noradrenaline to fibronectin: evidence for a general mechanism of monoaminylation. FEBS Lett. 2012; 586(19):3421–8. [PubMed: 22858378]
34. Liu Y, Wei L, Laskin DL, Fanburg BL. Role of protein transamidation in serotonin-induced proliferation and migration of pulmonary artery smooth muscle cells. Am J Respir Cell Mol Biol. 2011; 44(4):548–55. [PubMed: 20558776]
35. Dale GL, Friese P, Batar P, et al. Stimulated platelets use serotonin to enhance their retention of procoagulant proteins on the cell surface. Nature. 2002; 415(6868):175–9. [PubMed: 11805836]
36. Kalamajski S, Liu C, Tillgren V, et al. Increased C-telopeptide cross-linking of tendon type I collagen in fibromodulin-deficient mice. J Biol Chem. 2014; 289(27):18873–9. [PubMed: 24849606]
37. Eyre DR, Paz MA, Gallop PM. Cross-linking in collagen and elastin. Annu Rev Biochem. 1984; 53:717–48. [PubMed: 6148038]

38. Fessel G, Li Y, Diederich V, et al. Advanced glycation end-products reduce collagen molecular sliding to affect collagen fibril damage mechanisms but not stiffness. PLoS One. 2014; 9(11):e110948. [PubMed: 25364829]

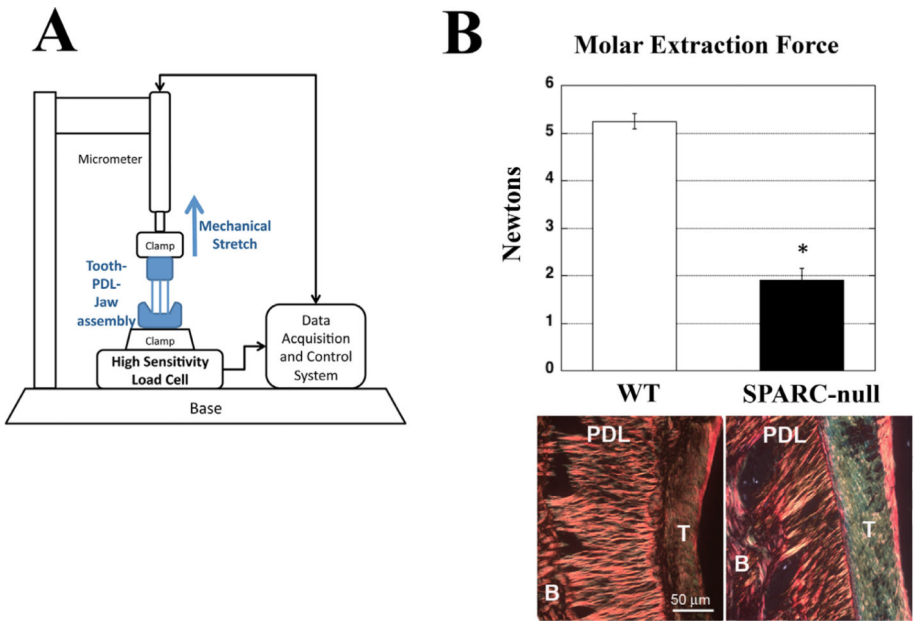

Fig. 1.

Molar extraction forces for SPARC-null teeth are significantly decreased in comparison to that of WT. (*A*) WT and SPARC-null first mandibular molars were extracted and the force of extraction was quantified using the assembly depicted. (*B*) SPARC-null molars (black bar) were extracted with significantly less force than WT molars (white bar), indicative of a decrease in the mechanical strength of the PDL in SPARC-null mice. Representative PSR-stained images of WT and SPARC-null PDL at 1 month are shown. *$p < 0.05$ between WT and SPARC-null, as determined by Student's *t* test. $n = 9$ mice per genotype. Error bars = SE. SPARC = secreted protein acidic and rich in cysteine; PDL = periodontal ligament; PSR = Picrosirius red; B = bone; T = tooth.

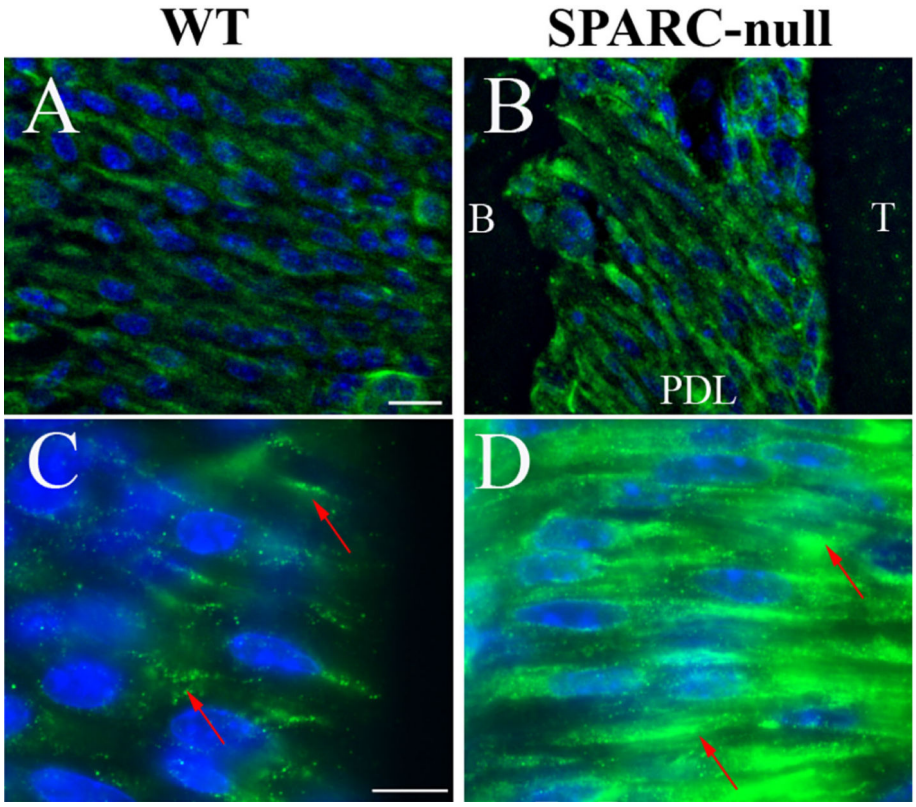

Fig. 2.

SPARC-null PDL exhibits increased intensity of N-ε-γ-glutamyl lysine immunoreactivity. WT (*A*, *C*) and SPARC-null (*B*, *D*) PDL sections were stained with an antibody against N-ε-γ-glutamyl lysine, the covalent cross-link formed by transglutaminase. Although both WT and SPARC-null PDL demonstrated positive staining, SPARC-null PDL sections showed apparent greater intensity of staining as compared to WT PDL. Higher magnifications (*C*, *D*) revealed that SPARC-null PDL had more intense patches of N-ε-γ-glutamyl lysine localization. Each image is orientated as indicated in *B* and is representative of $n = 3$ mice of each genotype at 4 months of age. Scale = 25 μm. SPARC = secreted protein acidic and rich in cysteine; PDL = periodontal ligament; B = bone; T = tooth.

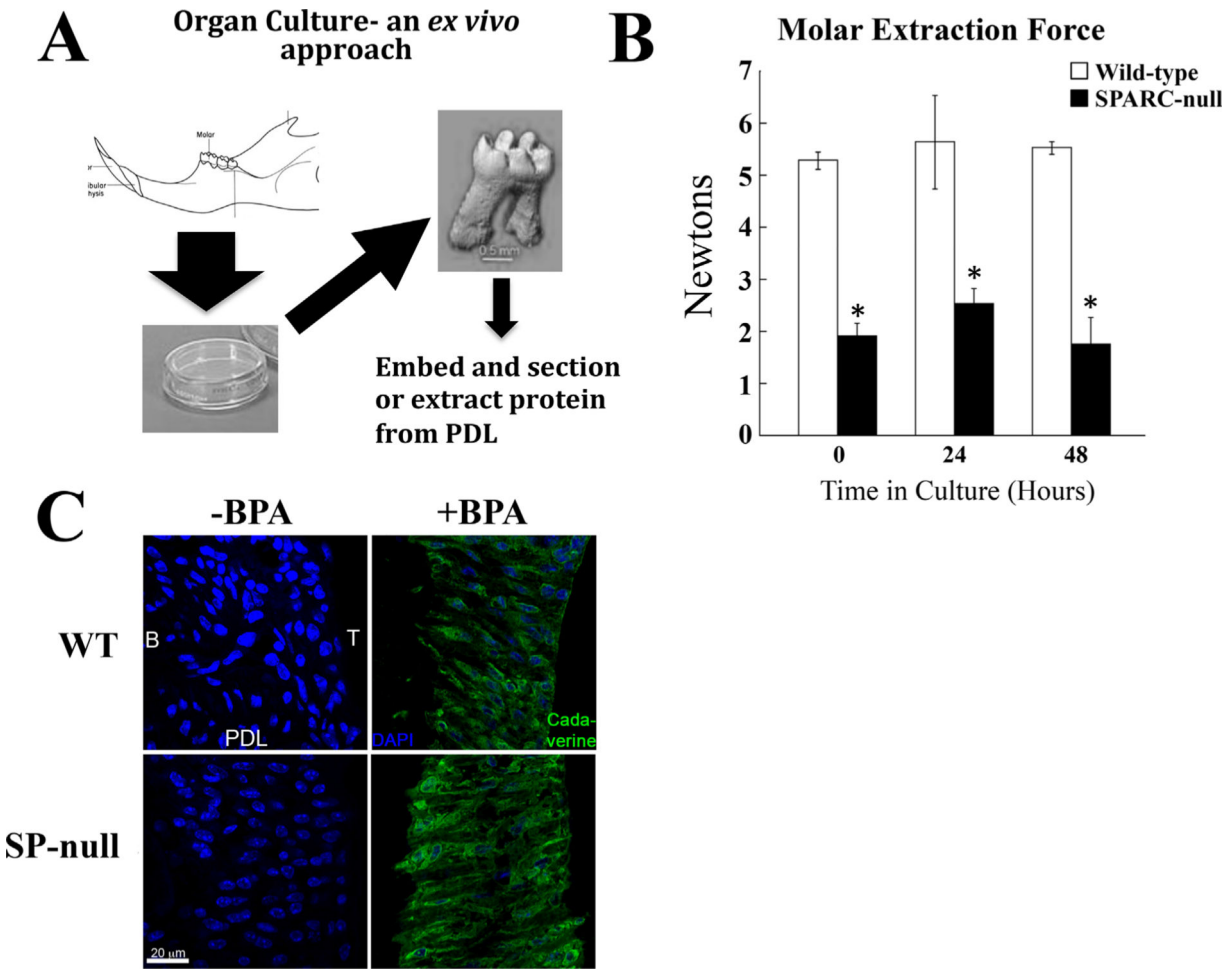

Fig. 3.

Organ cultures of WT and SPARC-null PDL maintain respective mechanical strength and BPA incorporation by transglutaminase. (*A*) To further characterize WT and SPARC-null PDL, an organ culture system was developed, as depicted. WT and SPARC-null mandibles were removed and cultured exvivo in growth media as described in Materials and Methods. (*B*) Mechanical testing of jaws incubated for 24 or 48 hours was carried out to establish that PDL maintained structure and integrity in organ culture. For comparison, the 0 hour time in Fig. 1 is provided. No significant differences in the molar extraction force were detected after 24 or 48 hours of culture within each genotype versus time 0. The molars of SPARC-null teeth continued to require reduced extraction forces versus that of WT teeth. $*p < 0.05$ between WT and SPARC-null at each isolated time point, by Student's *t* test. (*C*). Jaws incubated without BPA (–BPA), a pseudosubstrate of transglutaminase, and with BPA (+BPA), were fixed and sectioned. Staining with avidin-FITC demonstrated BPA incorporation (green) in both WT and SPARC-null PDL with no detectable localization in vehicle control samples (–BPA). SPARC-null sections had increased immunofluorescence intensity, in comparison to sections from WT PDL. DAPI stain of nuclei is shown as blue. Bar = 20 µm. SPARC = secreted protein acidic and rich in cysteine; PDL = periodontal ligament; B = bone; T = tooth; BPA = 5-(Biotinamido) pentylamine.

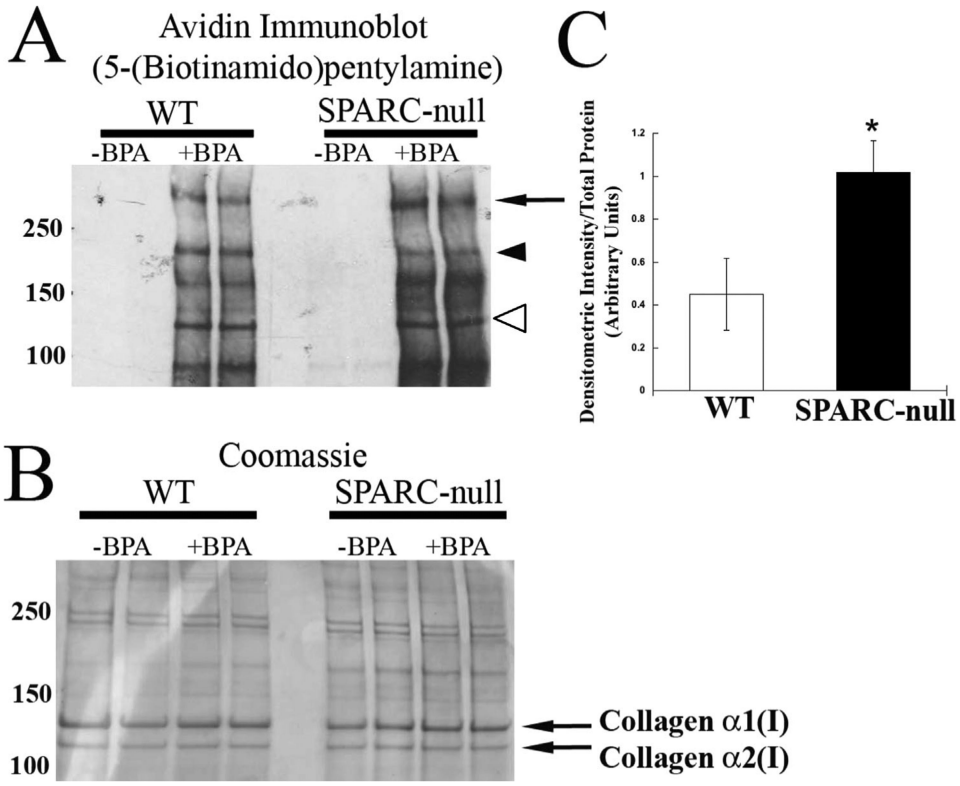

Fig. 4.

Transglutaminase-mediated BPA incorporation is increased in proteins extracted from SPARC-null PDL. (*A*) Western blot of SDS-PAGE separated PDL protein probed with avidin antibody to detect BPA incorporation. The arrowhead indicates a protein with increased BPA incorporation in a WT PDL, whereas the arrow indicates a protein band that has increased BPA incorporation in SPARC-null extracts. Open arrowhead indicates protein band with migration consistent with that of collagen α1(I). (*B*) Coomassie-blue–stained gel of proteins loaded in A to demonstrate equal loading of protein. (*C*) Proteins from SPARC-null PDL have increased incorporation of BPA, as quantified in independent organ culture experiments ($n = 4$). *$p < 0.05$ between WT and SPARC-null. SPARC = secreted protein acidic and rich in cysteine; PDL = periodontal ligament; B = bone; T = tooth; BPA = 5-(Biotinamido) pentylamine.

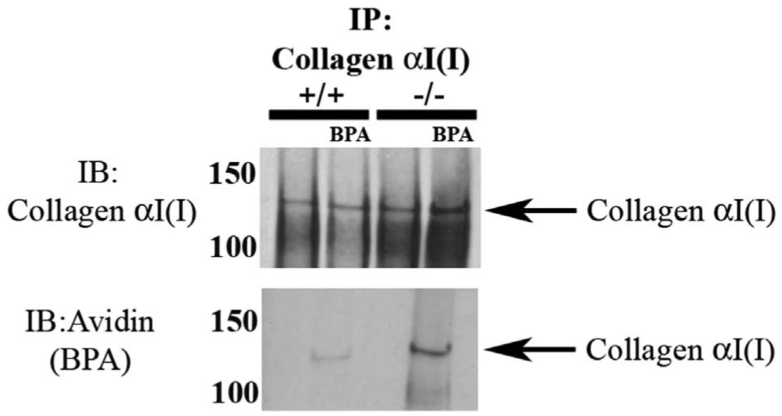

Fig. 5.

Collagen I pulled down from SPARC-null PDL proteins demonstrated increased BPA incorporation versus that in WT PDL extracts. Collagen α1 (I) pulled down from protein extracted from WT and SPARC-null PDL contained BPA-labeled collagen α1(I) (top). SPARC-null PDL collagen α1(I) exhibited increased BPA incorporation in comparison to WT PDL, when equal amounts of starting protein were used. Avidin-HRP Western blots of SPARC-null collagen α1(I) immunoprecipitation also revealed a secondary band, collagen α2(I), labeled with BPA, that was not detected in WT collagen α1(I) pull-downs. The results shown are representative of four independent experiments. BPA = 5-(Biotinamido) pentylamine; IP = immunoprecipitation; IB = immunoblot; HRP = horseradish peroxidase.

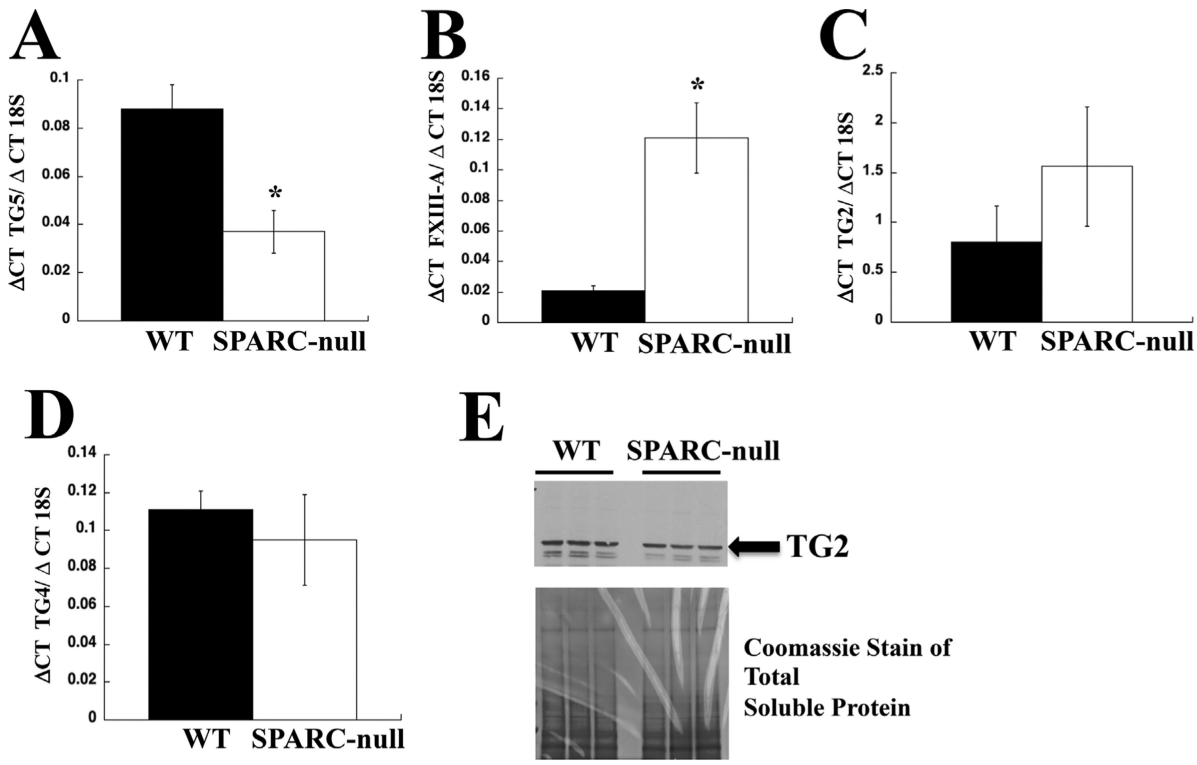

Fig. 6.

TGs expressed in PDL. RT-PCR with TG-specific primers (Supporting Table 1) was performed to detect expression of different TG family members in PDL. (*A*) Increased expression of mRNA encoding TG5 was detected in WT (black bars) versus SPARC-null (white bars). (*B*) In contrast, increased expression of Factor XIII-A was detected in SPARC-null (white bars) versus WT (black bars) in murine PDL samples. (*C*) No significant differences were detected in TG2 mRNA expression between WT (black bars) and SPARC-null (white bars) samples. (*D*) Similarly, no significant differences in TG4 were detected in WT versus SPARC-null PDL. (*E*) Western blot analysis of TG2 revealed similar levels of TG2 protein in WT and SPARC-null PDL extracts. Total soluble protein is shown as detected by Coomassie stain is shown as a loading control. *$p < 0.05$ between WT and SPARC-null. SPARC = secreted protein acidic and rich in cysteine; PDL = periodontal ligament; TG = transglutaminase.

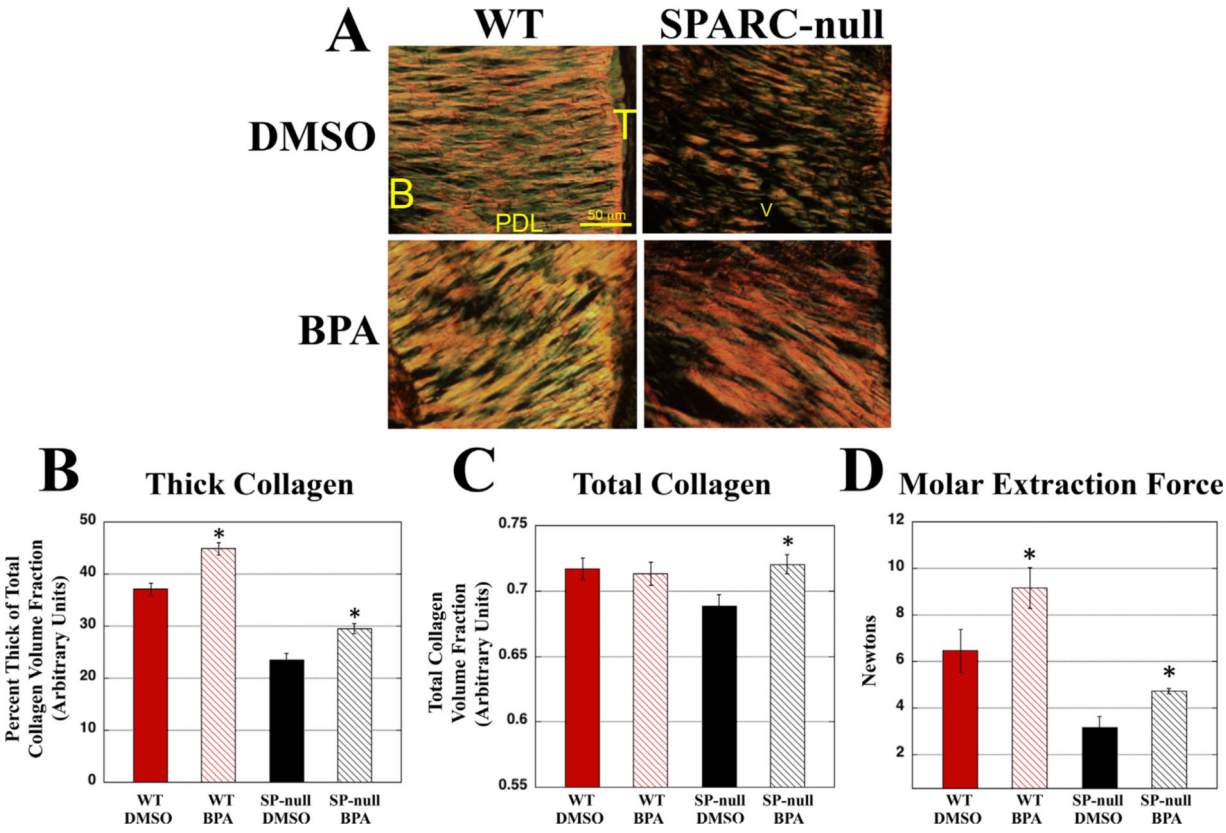

Fig. 7.

Injection of BPA restores collagen in SPARC-null PDL. (*A*) PSR-stained sections of either DMSO (Control, top panels) or BPA-injected (bottom panels) WT and SPARC-null PDL. BPA-injected SPARC-null PDL appeared to have an increase in thick collagen, as well as increases in total collagen over control sections. BPA-injected WT also had apparent increases in thick collagen. (*B*) WT and SPARC-null PDL had significant increases in the percent volume fraction of thick collagen following BPA injections versus control values. (*C*) In SPARC-null PDL, but not WT, BPA injection significantly increased total collagen volume fractions over that of control values. (*D*) The molar extraction force of WT and SPARC-null PDL was increased in BPA-injected mice versus vehicle control. *$p < 0.05$ between the DMSO injected and BPA injected for each genotype, $n = 8$ mice per genotype per condition for measurements of total collagen and fiber thickness, $n = 5$ mice per genotype for mechanical strength measurements. SPARC = SP = secreted protein acidic and rich in cysteine; PDL = periodontal ligament; PSR = Picrosirius red; B = bone; T = tooth; BPA = 5-(Biotinamido) pentylamine; DMSO = dimethylsulfoxide.